

An Embedded 3D Fracture Modeling Approach for Simulating Fracture-Dominated Fluid Flow and Heat Transfer in Geothermal Reservoirs

Cong Wang, Philip Winterfeld, Bud Johnston and Yu-Shu Wu

1600 Arapahoe St., Colorado School of Mines, Golden, CO, 80401

ywu@mines.edu

Keywords: Geothermal Reservoir, Reservoir Simulation, Fracture Simulation, EDFM

ABSTRACT

In this paper, we describe an efficient modeling approach, named embedded discrete fracture method (EDFM), for incorporating arbitrary 3D, discrete fractures, such as hydraulic fractures or faults, into modeling fracture-dominated fluid flow and heat transfer in fractured geothermal reservoirs. This technique allows 3D discrete fractures to be discretized independently from surrounding rock volume and inserted explicitly into a primary fracture/matrix grid, generated without including 3D discrete fractures in prior. An effective computational algorithm is developed to discretize these 3D discrete fractures and construct local connections between 3D fractures and fracture/matrix grid blocks representing the surrounding rock volume. The constructed gridding information on 3D fractures is then added to the primary grid. This embedded fracture modeling approach can be directly implemented into a developed geothermal reservoir simulator via the integral finite difference (IFD) method or with TOUGH2 technology. This embedded fracture modeling approach is very promising and computationally efficient to handle realistic 3D discrete fractures with complicated geometries, connections, and spatial distributions. Compared with other fracture modeling approaches, it avoids cumbersome 3D unstructured, local refining procedures, and increases computational efficiency by simplifying Jacobian matrix size and sparsity, while maintaining sufficient accuracy. Several numerical simulations are presented to demonstrate the utility and robustness of the proposed technique. Our numerical experiments show that this approach captures all the key patterns about fluid flow and heat transfer dominated by fractures in these cases. Thus, this approach is readily available to simulation of fractured geothermal reservoirs with both artificial and natural fractures. NREL and CSM are participants in EGS Collab, which is led by Lawrence Berkley National Laboratory (LBNL). The NREL/CSM EGS Collab team intends to implement EDFM into TOUGH2-EGS to history match circulation tests.

1. INTRODUCTION

Geothermal energy is a clean and sustainable energy source, which deals with the heat energy generated and stored within the earth. It includes three major types: the hydrothermal source, the geo-pressured source, and sources stored in hot, dry rocks. The third type, hot, dry rock, is by far the most abundant source of geothermal energy available to mankind. These systems are fluid independent, which involve non-porous and impermeable rocks where the temperature is high enough to be useful. The essential step to develop this system is creating a fracture system (either by high pressure hydraulic fracturing to create new fractures over a very short period of time or by the shear reactivation of pre-existing fracture at relatively low pressure just high enough to cause shear failure over a long-time period), and then completing a circulation loop by drilling another well that intersects the hydraulic fracture region. Freshwater is injected from one well, forcing it to flow through the fracture, and then is produced from the other well. In this process, the thermal energy is extracted by the heat conduction when the water is exposed to hot rock surfaces.

Reservoir simulation provides a practical approach to characterize key reservoir parameters in this process (such as temperature, permeability, thermal and hydrologic structures), improve our understandings of such geothermal reservoirs, and evaluate/optimize geothermal utilization scheme. Reservoir simulators are built based on sound physical laws about fluid flow and heat transfer and employ mathematical and numerical techniques to quantify these phenomena. Currently there are several geothermal simulators available to simulate the complicated coupling process between mass and energy transport in a geothermal reservoir, such as SHAFT79 (Pruess and Schroeder 1980), MULKOM (Pruess and Wu 1988), TOUGH2 (Pruess et al. 1999), TAURUS (Settari and Walters 2001), STARS (Computer Modeling Group Ltd 2012), ECLIPSE (SCHLUMBERGER 2009). The simulations studied here were carried out with TOUGH2-EGS (Fakcharoenphol et al. 2013), which belongs to the TOUGH2 family and can simulate the coupled thermal-hydraulic-mechanical-chemical (THMC) process.

For the simulation of hot, dry rock geothermal reservoirs, the key is handling the 2D fluid flow and heat transfer within the large-scale hydraulic fractures, which is coupled to the transient heat conduction equation for surrounding rocks. Traditional modeling techniques to quantify fluid flow and heat transfer with fractures can be divided into two major categories. The first one is the multiple-continua method. Classical double-porosity, double-permeability, and MINC all belong in this category (Warren and Root 1963; Kazemi 1969; Duguid and Lee 1977; Pruess et al. 1999; Wu et al. 2007). In this approach, fracture and matrix are conceptualized as two independent continua which are overlaid with each other. Local interactions between the fracture and matrix are captured by the analytical solution based on the pseudo-steady state assumption. This approach can only capture some key features (such as fracture spacing and characteristic length) while neglecting details of fracture geometry and locations, because it assumes fractures are uniformly distributed in the whole reservoir. Therefore, it is not applicable for reservoir simulations with dominant fractures, e.g., hydraulic fractures in hot, dry rocks. The second approach is the explicit fracture modeling. The first technique in this approach is based on structured grids, in

which fractures are represented by a series of small-scale grids (Slough et al. 1999; Sadrpanah et al. 2006). This technique could only model fractures with regular shape and with directions along the principal axis. The second technique is based on unstructured grids. The unstructured grids are constructed in a way that grid edges/faces coincide with the fracture (Karimi-Fard et al. 2003; Sun and Schechter 2014). This technique is general, but constructing such unstructured grids is cumbersome, especially for complicated fractures in three dimensions.

In this paper, we describe an efficient modeling approach, named embedded discrete fracture method (EDFM), for incorporating arbitrary 3D, discrete fractures, such as hydraulic fractures or faults, into modeling fracture-dominated fluid flow and heat transfer in fractured geothermal reservoirs. This technique allows 3D discrete fractures to be discretized independently from surrounding rock volume and inserted explicitly into a primary fracture/matrix grid, generated without including 3D discrete fractures in prior. An effective computational algorithm is developed to discretize these 3D discrete fractures and construct local connections between 3D fractures and fracture/matrix grid blocks of representing the surrounding rock volume. The constructed gridding information on 3D fractures is then added to the primary grid. This embedded fracture modeling approach can be directly implemented into a developed geothermal reservoir simulator via the integral finite difference (IFD) method or with TOUGH2 technology. This embedded fracture modeling approach is very promising and computationally efficient to handle realistic 3D discrete fractures with complicated geometries, connections, and spatial distributions. Compared with other fracture modeling approaches, it avoids cumbersome 3D unstructured, local refining procedures, and increases computational efficiency by simplifying Jacobian matrix size and sparsity, while keeps sufficient accuracy. Several numerical simulations are presented to demonstrate the utility and robustness of the proposed technique. Our numerical experiments show that this approach captures all the key patterns about fluid flow and heat transfer dominated by fractures in these cases. Thus, this approach is readily available to simulation of fractured geothermal reservoirs with both artificial and natural fractures. This paper is organized as follows. Governing equations are briefly introduced in Section 2. In Section 3, key techniques to realize the EDFM and its accuracy evaluations are described. In Section 4, two typical problems are simulated to validate the accuracy of our developed EDFM models. In Section 5, we performed a numerical modeling study with EDFM to history match the performance of a hot dry rock geothermal reservoir, simulated scenarios with complicated fracture systems, and conducted sensitivity analysis about the production temperature with respect to the injection rate, the heat conductivity, and the specific heat.

2. GOVERNING EQUATIONS

The mathematical and numerical framework starts from the integral form of mass and energy balance equations of describing fluid and heat flow in a multi-phase, multi-component system (Pruess et al. 1999; Fakcharoenphol et al. 2013):

$$\frac{d}{dt} \int_{V_n} \mathbf{M}^\kappa dV_n = \int_{\Gamma_n} \mathbf{F}^\kappa \cdot \mathbf{n} d\Gamma_n + \int_{V_n} \mathbf{q}^\kappa dV_n \quad (1.1)$$

where V_n is an arbitrary subdomain for integration bounded by the close surface Γ_n ; the quantity \mathbf{M} , \mathbf{F} , and \mathbf{q} denote the accumulation term (mass or energy per volume), the flux term, and sink/source term, respectively; \mathbf{n} is a normal vector on subdomain surface pointing inward into the element; the superscript κ represents one component; and the subscript n denotes one grid blocks.

The general form of the mass accumulation term is:

$$\mathbf{M}^\kappa = \sum \phi S_\beta \rho_\beta X_\beta^\kappa \quad (1.2)$$

where ϕ is the effective porosity, ρ_β is the density of phase β , S_β is the phase saturation, X_β^κ is the mole fraction of component κ in phase β .

The heat accumulation term consists of contributions from the rock matrix, liquid phases. It is given by equation:

$$\mathbf{M}^\kappa = (1 - \phi) \rho_R C_R T + \phi \sum_\beta S_\beta \rho_\beta u_\beta \quad (1.3)$$

where ρ_R and C_R are grain density and specific heat of the host rock respectively, T is the temperature, and u_β is the specific internal energy in phase β .

In the mass flux term, \mathbf{F}^κ is the advective mass flux summing over phases:

$$\mathbf{F}^\kappa = \sum_\beta X_\beta^\kappa \mathbf{F}_\beta \quad (1.4)$$

where \mathbf{F}_β can be expressed by the multiphase extension of Darcy's law:

$$\mathbf{F}_\beta = -k_0 \frac{k_{r\beta} \rho_\beta}{\mu_\beta} (\nabla P_\beta - \rho_\beta \mathbf{g}) \quad (1.5)$$

where k_0 is the absolute permeability, $k_{r\beta}$ is the relative permeability to phase β , μ_β is the viscosity, P_β is the pressure in β phase, and \mathbf{g} is the vector of gravitational acceleration.

The heat flux term accounts for the conduction and advection heat transfer and is given by:

$$\mathbf{F}^k = - \left[(1 - \phi) K_R + \phi \sum_\beta S_\beta K_\beta \right] \nabla T + \sum_\beta h_\beta \mathbf{F}_\beta \quad (1.6)$$

where K_R is the thermal conductivity of the rock, K_β is thermal conductivity of the fluid phase β , and h_β is the specific enthalpy of phase β .

3. EDFM

The embedded discrete fracture method (EDFM) is a numerical technique to handle fluid flow and heat transfer in porous media with discontinued fractures (Lee et al. 2001; Moifar et al. 2014; Wang et al. 2017). As its name implies, fractures are virtually embedded into matrix grid blocks. The interactions between fractures and its surrounding matrix are accounted via the geometrical calculation. This can be explained by the discretized form of the mass flux term in Eq. (1.1).

$$\int_{\Gamma_n} \mathbf{F}_\beta \cdot \mathbf{n} d\Gamma_n = \sum_{j \in \eta_i} (\bar{\rho}_\beta \lambda_\beta)_{ij+1/2}^{n+1} \gamma_{ij} [\Phi_{\beta j}^{n+1} - \Phi_{\beta j}^n] \quad (1.7)$$

where η_i contains the set of neighbor elements to which element i is directly connected; $\Phi_{\beta j}$ denotes the potential of fluid phase β in node j ; and λ_β is the mobility of phase β ;

$$\lambda_\beta = \frac{k_{r\beta}}{\mu_\beta} \quad (1.8)$$

and the transmissivity of flow terms is defined as

$$\gamma_{ij} = \frac{A_{ij} k_{ij+1/2}}{d_i + d_j} \quad (1.9)$$

where A_{ij} is the common interface area between the intersected block and the fracture; d_i and d_j are distances from center of each block to the common interface; $k_{ij+1/2}$ is an averaged (such as harmonic-weighted) absolute permeability.

The key to incorporate the fracture-matrix interactions through the EDFM is obtaining the contact area and the average distance between the virtually embedded fracture element and its surrounding matrix grid blocks. Such geometric calculation is straightforward for 2D or 2.5D cases, but it is challenging for 3D cases. Table 1 summarizes key steps of the algorithm to calculate the intersection between a plane and a 3D cube. We also discussed some auxiliary techniques to handle fractures with infinite or finite conductivities, as well as multiple connected fractures.

Table 1 Procedures to calculate 3D box and plane intersections

Algorithm Calculating 3D Box and Plane Intersection	
1:	Process begins;
2:	Find all vertices of the intersected polygon;
3:	Check if one or more of the fracture polygon points are inside the box;
4:	Check if any of the box edges are intersected with the fracture polygon face;
5:	Check if any of the fracture polygon's edges are intersected with the box faces;
6:	Merge duplicates on the vertex list (if the plane crosses exactly the box corner);
7:	if (Vertex Number) > 2 then
8:	Sort vertices in the clockwise or counter-clockwise order;
9:	Calculate the area and the average distance of the intersected polygon;
10:	else
11:	No effective intersection between the polygon and the box;
12:	end if

The accuracy of the EDFM is evaluated by comparing its assumptions with analytical-solution based parameters. Our quantitative analysis indicates that the EDFM cannot provide solutions with unconditional accuracy. The numerical error comes from the simplification in handling local interactions between the fracture and its surrounding matrix grid blocks. For some extreme cases, this numerical error could be significant. However, we also find that this numerical error can be mitigated if the local matrix grid blocks are properly refined. We provide an analytical-solution based method to optimize this local grid refinement size if needed.

Consider governing equations of both the heat conduction and fluid flow in the porous medium, which share the following form:

$$\frac{\partial u}{\partial t} - \alpha \nabla^2 u = 0 \quad (1.10)$$

In the heat equation, u denotes the temperature, and α is the thermal diffusivity; in the equation describing fluid flow through porous medium, u denotes the pressure, and α is the diffusivity. The definition of α is following:

$$\alpha = \begin{cases} k_t / (c_p \rho), & \text{heat transfer} \\ k_f / (\phi \mu c_t), & \text{fluid flow} \end{cases} \quad (1.11)$$

where k_t is the thermal conductivity; c_p is the specific heat capacity; ρ is the mass density of the material;

k_f is the permeability; ϕ is the porosity; μ is the fluid viscosity; and c_t is the total compressibility.

We solve Eq. (1.10) analytically for a 1D problem with a constant fracture pressure condition (Dirichlet condition) on the right and with a closed boundary condition (Neumann condition) applied on the left (Wang et al. 2017). This analytical solution gives us the accurate evaluation of the average distance between the fracture and its surrounding matrix grid blocks, as shown in Eq. (1.12). The average distance according to the EDFM is given in Eq. (1.13).

$$d_{m-f} = \frac{x_L^2 \sum_{n=1}^{\infty} \frac{1}{(n-0.5)^2} \left(1 - \cos \left[(n-0.5) \pi \frac{\Delta x_1}{x_L} \right] \right) \exp \left[-(n-0.5)^2 \pi^2 \frac{\alpha}{x_L^2} t \right]}{\Delta x_1 \pi^2 \sum_{n=1}^{\infty} \exp \left[-(n-0.5)^2 \pi^2 \frac{\alpha}{x_L^2} t \right]} \quad (1.12)$$

$$d_{m-g} = \frac{\Delta x_1}{2} \quad (1.13)$$

From Eq. (1.12), the accurate (analytical-solution based) average distance depends on the grid size, time and the diffusivity value. We plot the relative error between these two average distances, as defined in Eq. (1.14), with various grid sizes (1 m ~ 10 m), diffusivity values ($1.0 \times 10^{-5} \text{ m}^2 / \text{s} \sim 1.0 \times 10^{-1} \text{ m}^2 / \text{s}$) and time steps (1 min, 1 hour and 1 day). Results of this analysis are plotted in

$$\text{RE} = \frac{|d_{m-g} - d_{m-f}|}{d_{m-f}} \quad (1.14)$$

As observed in these figures (Figure 1 - Figure 3), the relative error decreases with the decrease of the grid size, with the increase of the time step, and with the increase of the diffusivity value. This indicates that the computational error can be mitigated by controlling the size of grids which contain fractures in the EDFM. For most of practical geothermal simulation problems, the value of thermal diffusivity is in the range between $1.0 \times 10^{-5} \text{ m}^2 / \text{s}$ and $1.0 \times 10^{-4} \text{ m}^2 / \text{s}$, while the value of diffusivity regarding the fluid flow in the porous medium is in the range between $1.0 \times 10^{-4} \text{ m}^2 / \text{s}$ and $1.0 \times 10^{-1} \text{ m}^2 / \text{s}$.

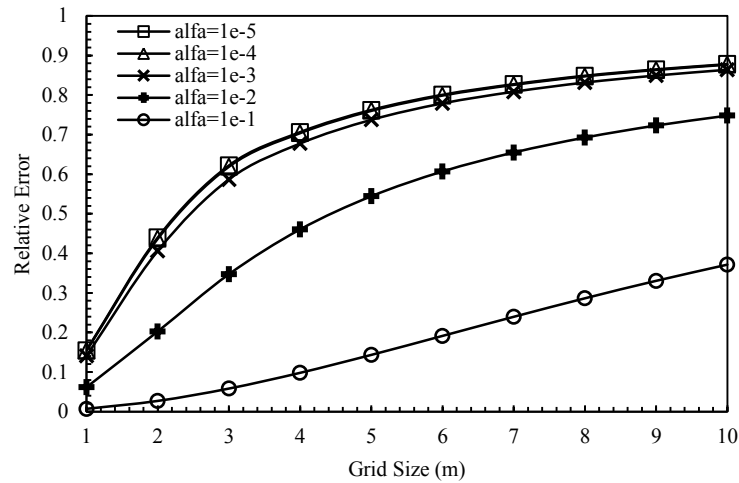


Figure 1 Relative error with various grid sizes and diffusivities with a time step of 1 min

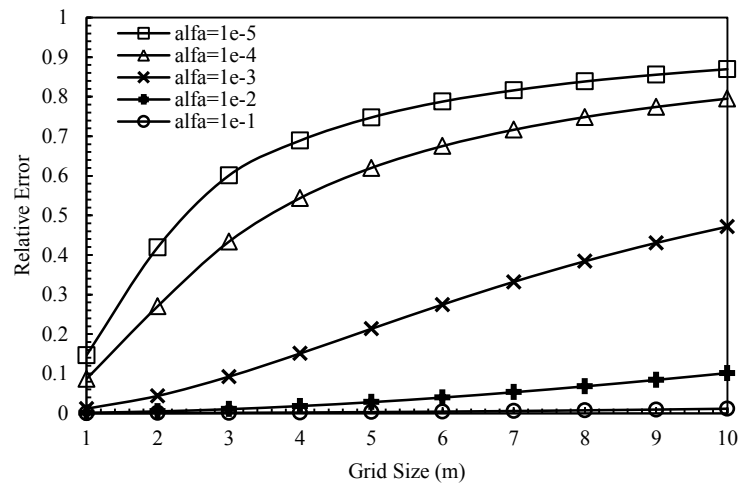


Figure 2 Relative error with various grid sizes and diffusivities with a time step of 1 hour

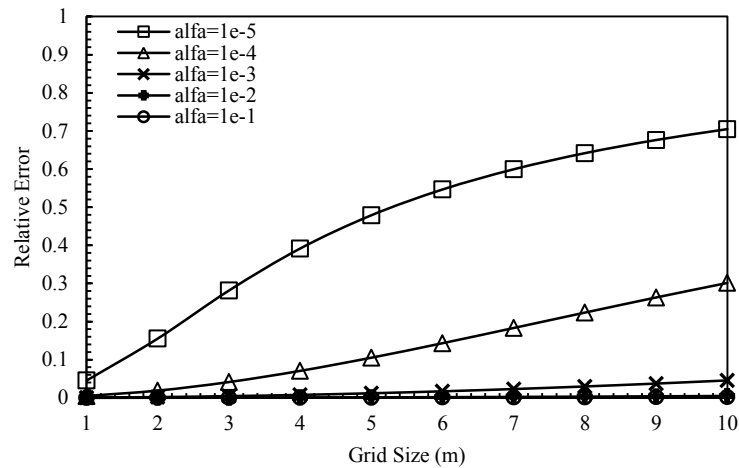


Figure 3 Relative error with various grid sizes and diffusivities with a time step of 1 day

4. VALIDATIONS

This is to examine the accuracy of the EDFM in simulating fluid flow and heat transfer with fractures. The problem concerns fluid flow and heat transfer across a horizontal fracture, which is bounded by impermeable rocks. The mechanical and chemical processes are beyond the scope of this study. The system contains single-phase isothermal water at initial, and a constant water mass injection rate with a colder temperature is imposed at the inlet of the fracture. The outlet end of the fracture is kept at a constant pressure. Table 2 summarizes parameters used in the simulation.

Table 2 Parameters and values for EDFM validations

Properties	Value	Unit
Rock		
Density	2650	kg/m ³
Heat conductivity	5.1	W/(m°C)
Specific heat	1000	J/(kg°C)
Permeability	0	m ²
Porosity	0.00	
Fracture		
Permeability	2.00E-10	m ²
Porosity	0.5	
Width	0.04	m
Initial Conditions		
Temperature	300	°C
Pressure	1.00E+07	Pa
Injection		
Temperature	100	°C
Rate	0.5	kg/s
Production		
Flowing BHP	1.00E+07	Pa

We studied two scenarios (considering and not considering heat supplies from surrounding rocks) with two numerical approaches. In the first approach, only fractures are included in the numerical model through an explicit approach, and the heat interaction between the fracture and its surrounding rocks is incorporated by approximate analytical solutions (Vinsome and Westerveld 1980; Pruess et al. 1999). In the second approach, both the fracture and its surrounding rocks are included in the numerical setup. The fracture is handled by the EDFM.

Figure 4 presents simulation results of the outlet temperature vs. time for these four cases. It's observed that results based on the EDFM have a good agreement with semi-analytical solutions for both scenarios. The case with no supplies of heat from surrounding rocks has an early thermal breakthrough time and a faster temperature decreasing rate afterward.

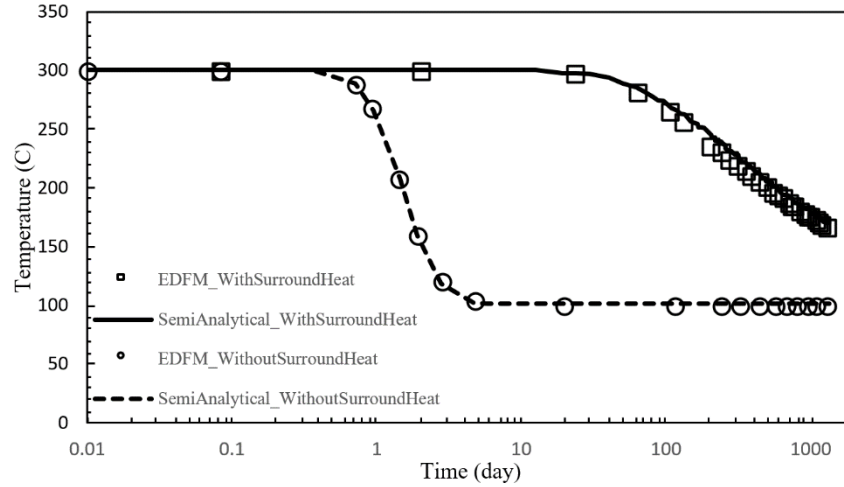


Figure 4 The outlet temperature fro two scenarios by EDFM and by semi-analytical approach

5. APPLICATIONS

The case study in this section is based on a project initiated at the Los Alamos Scientific Laboratory to investigate the feasibility of extracting energy from the hot, dry rock. Its detailed descriptions can be found in previous open literature (Murphy 1979; Dash et al. 1983). Here, we give brief information related to the application in this paper. This project locates at Fenton Hill in the Jemez Mountains of northern New Mexico. A geothermal reservoir is formed by hydraulic fracturing a hot, non-porous granite at 2.81 km in depth. Since the granitic rock is relatively homogeneous and unstratified, the hydraulic fracture can be assumed to be approximately circular in shape. The temperature at this site is 197 °C, with a geothermal heat flow of 0.16 W/m² (2.5 times the world average). The circulation loop is created by drilling two wells (one injection well and one production well) intersecting the hydraulic fracture region, and the fracture acts as the flow short-circuit between the injection and production wells. The injection point is located at the bottom of the fracture. The production well connects with two existing points inside the fracture at the shallower depth according to the temperature and radioactive tracer surveys. This injection/production system is schematically illustrated in Figure 5. The water alone, with no additives or propping agents, are used to extract heat from this reservoir by the heat conduction when the water is exposed to hot rock surfaces. Because the surrounding granite rocks are almost non-porous and impermeable, less than 1% of the injected water is lost outside the fracture.

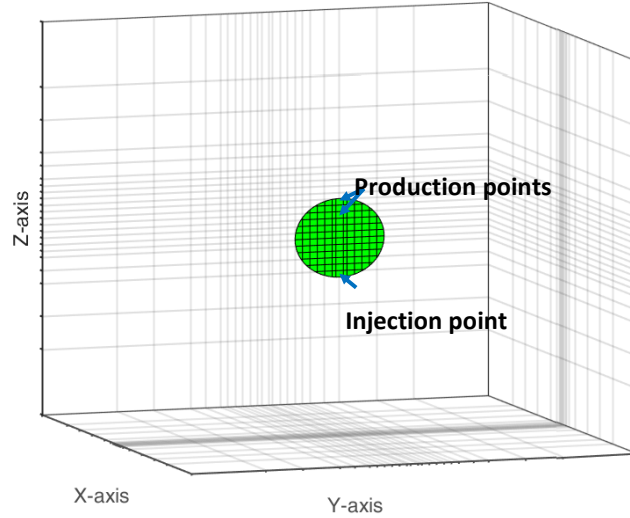


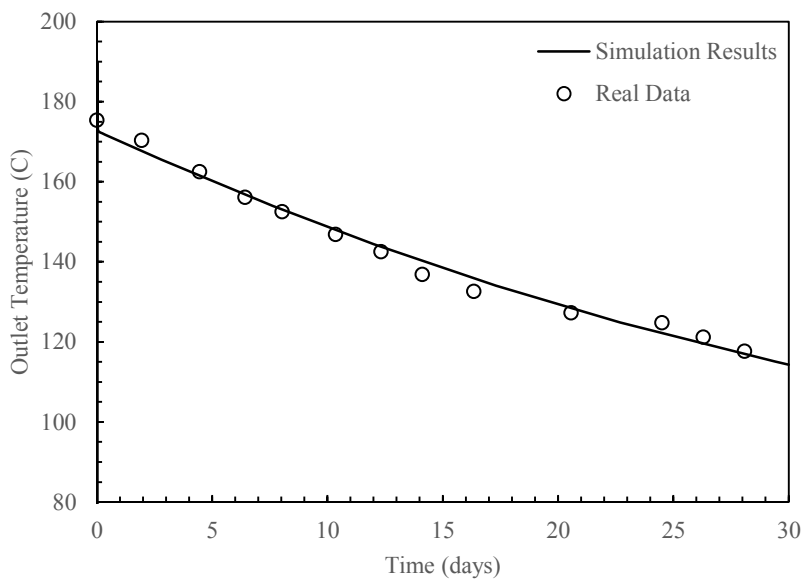
Figure 5 Schematic review of the fracture, injection point and production points in the case study

Injection flow rates and production temperatures were measured by surveying tools. Figure 6 presents the recorded temperature variation with time in the production well for the first 30 days. The corresponding injection flow rate keeps constant at $7.5 \times 10^{-3} \text{ m}^3/\text{s}$. We performed a numerical modeling study to history match the performance of this geothermal reservoir. In the basic model setup, the reservoir is assumed to be rectangular with dimensions of $600 \text{ m} \times 600 \text{ m} \times 600 \text{ m}$. Though a realistic reservoir extent may be larger, we considered it appropriate to simplify calculations by modeling a smaller domain of only 600 m in vertical and lateral extent. The computational mesh is three-dimensional and contains $19 \times 23 \times 22$ gridblocks, which are nonuniform with refinement around the fracture edge to capture the fracture geometry (Figure 5). The circular fracture is embedded into the original grids, leading to 9,758 computational grids (9,614 matrix grids and 144 fracture grids), and 27,888 computational connections (27,481 matrix-matrix connections, 144 matrix-fracture connections, and 263 fracture-fracture connections). In this history matching, three sets of adjustable parameters were used: the fracture radius, the fracture width and the injection temperature. These parameters were adjusted until simulation results matched observed production temperature data. Table 3 summarizes parameters used in the simulations for the final match. As demonstrated in Figure 6, simulation results of the case with a fracture radius of 60 m, the fracture aperture of 0.002 m and the injection temperature of $25 \text{ }^\circ\text{C}$ agree remarkably well with the field recorded data. Temperature of the production rate declines rapidly in this case. It takes 30 days for the temperature to decrease from $175 \text{ }^\circ\text{C}$ to $114 \text{ }^\circ\text{C}$. Parameter values from this history matching are close to previous characterizations of this geothermal reservoir as described in literature.

Figure 7 plots simulated production rates and production temperatures from these two outlets. The first outlet (the one close to the injection point) transmits approximately 70% of the flow, while the second transmits about 30%. Temperature of the production fluids drops faster in the first outlet. The mixed-mean fluid temperature, required for comparisons with measurements, is calculated as the sum of the product of the flow fraction and the computed temperature for the positions corresponding to the two communicating joints. Figure 8 plots the temperature contour inside this fracture after 30 days.

Table 3 Parameters and values in the case study

Properties	Value	Unit
Rock		
Density	2650	kg/m ³
Heat conductivity	3.9	W/(m°C)
Specific heat	750	J/(kg°C)
Permeability	0	m ²
Porosity	0.00	
Fracture		
Permeability	2.00E-10	m ²
Porosity	0.5	
Width	0.002	m
Radius	60	m
Initial Conditions		
Temperature	190	°C
Pressure	1.00E+07	Pa
Injection		
Temperature	25	°C
Rate	7.5	kg/s
Production		
Flowing BHP	1.00E+07	Pa

**Figure 6 History matching between the simulation result and field-recorded temperature data**

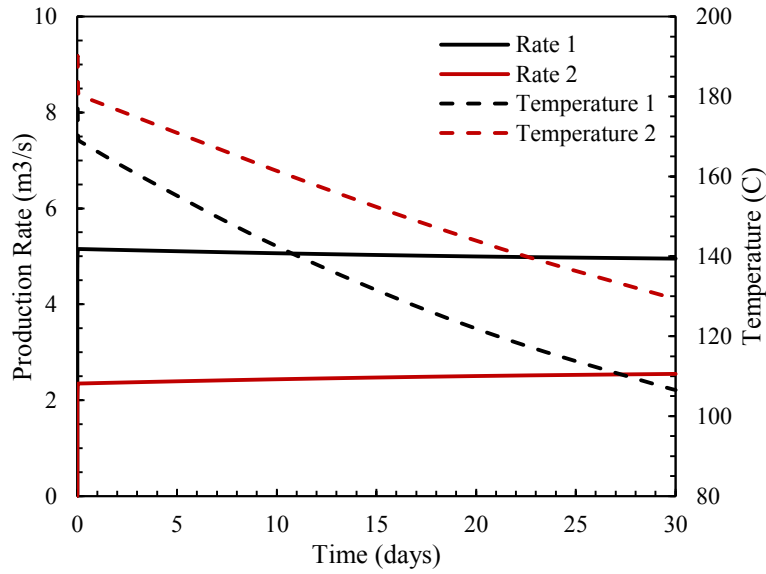


Figure 7 Production rates and temperatures at two outlets

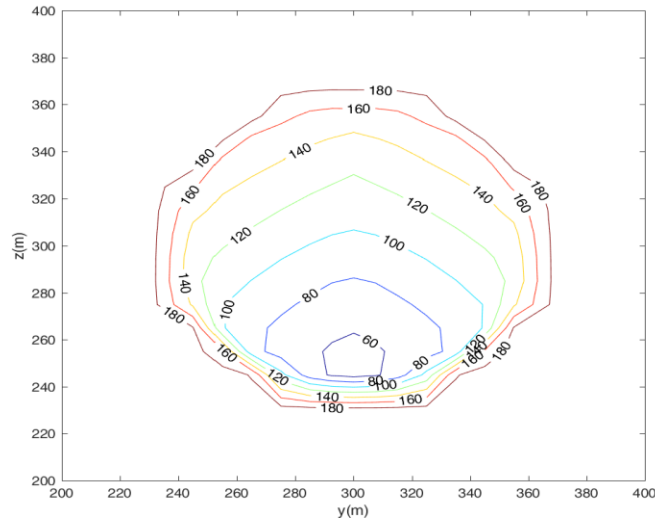


Figure 8 Temperature contour inside the fracture after injection of 30 days

Next, we simulate the same geothermal reservoir with a more complicated fracture system. The reservoir is enlarged by extending another vertical hydraulic fracture. These two vertical hydraulic fractures are connected by three nonvertical natural fractures with a dip of about 60° from horizontal. The effective heat-transfer area is thus significantly increased by considering both the second hydraulic fracture and natural fractures. The fracture geometry is interpreted conceptually from previous studies. Its numerical implementation through the EDFM is illustrated in the right part of Figure 9. All other reservoir properties keep the same with the one described above. Figure 10 and Figure 11 show the simulated temperature distribution at one month and one year in formations (horizontal slices) and in two vertical hydraulic fractures (vertical slices), respectively. Simulation results reveal our physical understandings qualitatively. The temperature in the inner reservoir part (the portion between two vertical fracture) drops faster than that in the outer reservoir part.

We further conducted six other numerical tests to investigate the sensitivity of production temperature with respect to the injection rate, the heat conductivity and the specific heat. The results from the sensitivity analysis are presented in Figure 12 - Figure 14. It indicates that the injection rate has the most significant impact among these three variables on production temperature. The impact of the heat conductivity on the production temperature is slight. Increasing or decreasing the heat conductivity by 50% only leads to about 1.5% change in the production temperature. The impact of the specific heat on the production temperature is negligible.

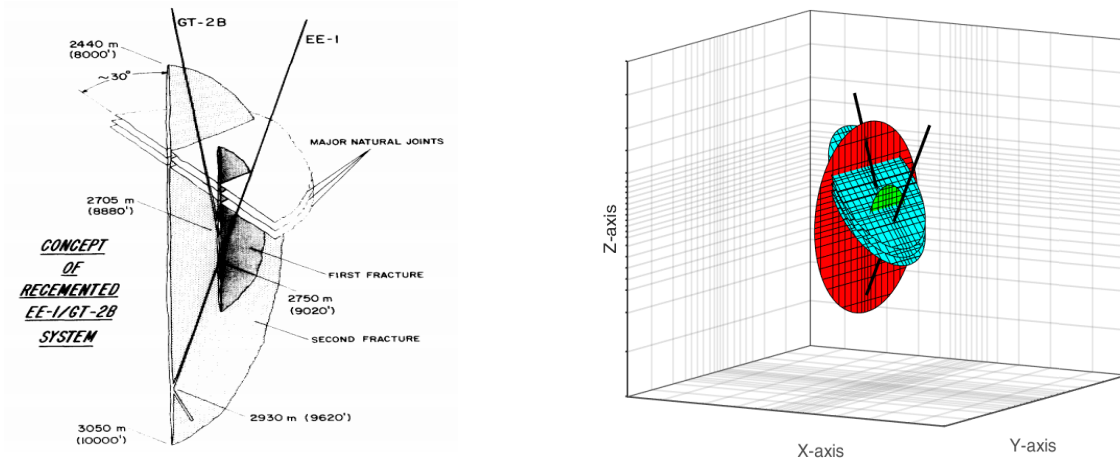


Figure 9 Interpreted fracture geometry from previous studies (Dash et al. 1983) and the numerical implementation by EDFM

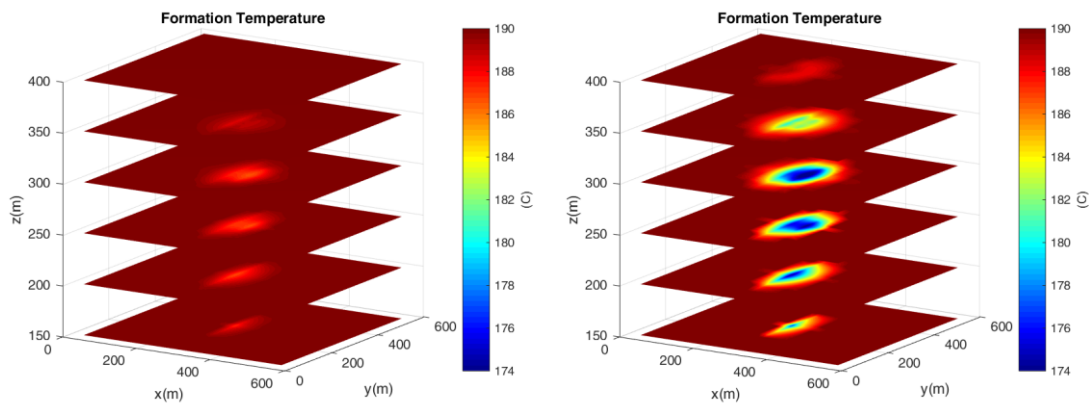


Figure 10 Temperature distributions in formations at 1 month and 1 year

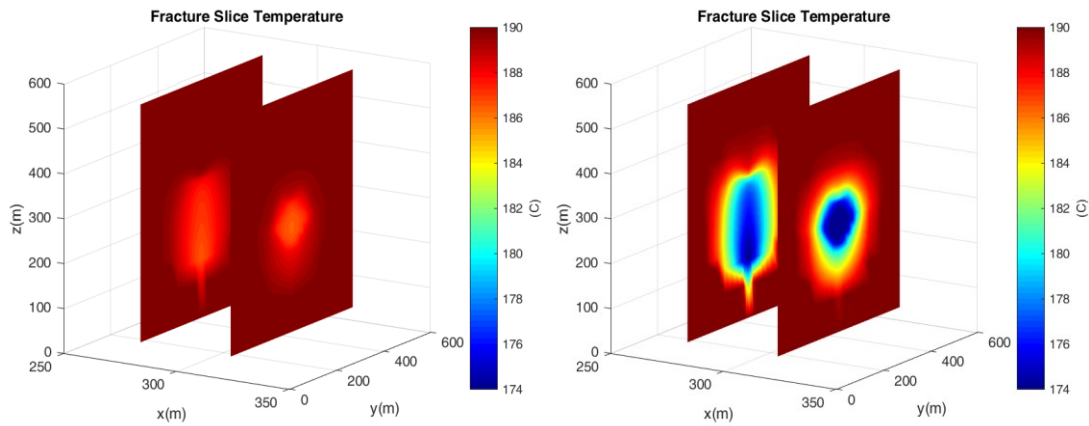


Figure 11 Temperature distributions in fractures at 1 month and 1 year

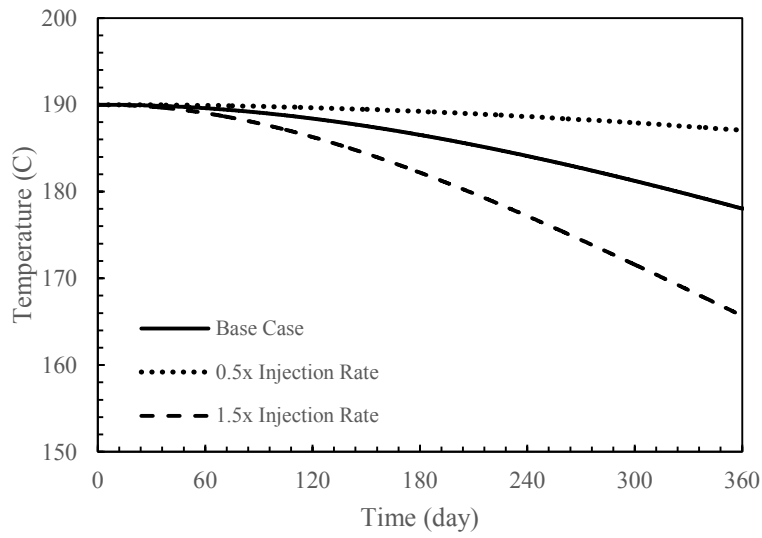


Figure 12 Sensitivity analysis of the production temperature with respect to the injection rate

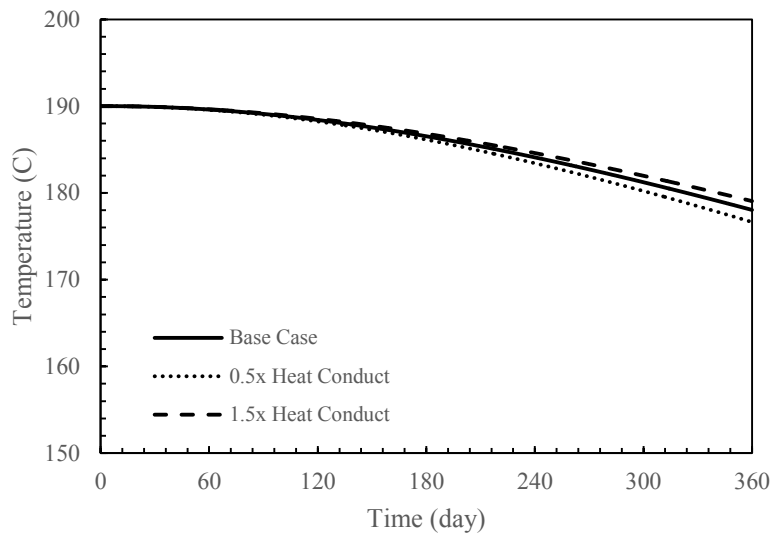


Figure 13 Sensitivity analysis of the production temperature with respect to the heat conductivity

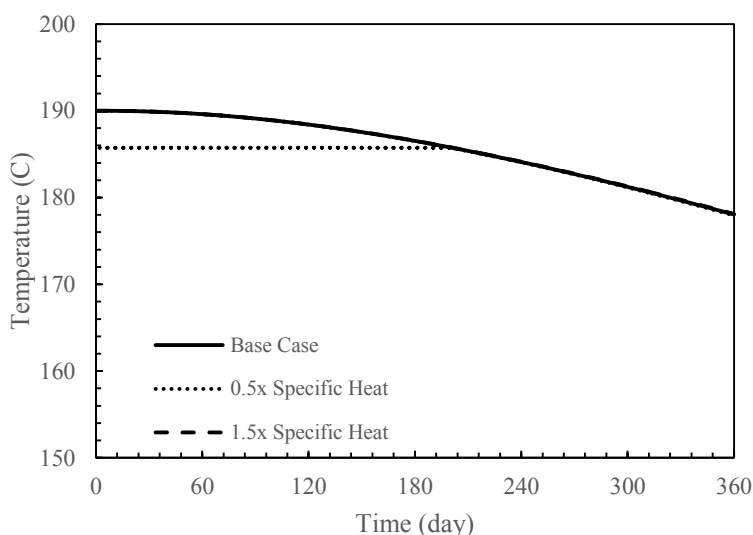


Figure 14 Sensitivity analysis of the production temperature with respect to the specific heat

CONCLUSIONS

We describe an efficient modeling approach, named embedded discrete fracture method (EDFM), for incorporating arbitrary 3D, discrete fractures, such as hydraulic fractures or faults, into modeling fracture-dominated fluid flow and heat transfer in fractured geothermal reservoirs. Compared with other fracture modeling approaches, it avoids cumbersome 3D unstructured, local refining procedures, and increases computational efficiency by simplifying Jacobian matrix size and sparsity, while keeps sufficient accuracy. Several numerical simulations are present to demonstrate the utility and robustness of the proposed technique. Our numerical experiments show that this approach captures all the key patterns about fluid flow and heat transfer dominated by fractures in these cases. Thus, this approach is readily available to simulation of fractured geothermal reservoirs with both artificial and natural fractures.

ACKNOWLEDGEMENT

This work was supported in part by EMG Research Center in Petroleum Engineering Department at Colorado School of Mines; and by Foundation CMG. Also, a portion of this research was supported by the U.S. Department of Energy, Office of Energy Efficiency and Renewable Energy (EERE), Geothermal Technologies Office (GTO) under Contract No.DE-AC36-08-GO28308 with the National Renewable Energy Laboratory as part of the EGS Collab project.

REFERENCES

- Dash, Z. V., H. D. Murphy, R. L. Aamodt, R. G. Aguilar, D. W. Brown, D. A. Counce, H. N. Fisher, et al. 1983. "Hot Dry Rock Geothermal Reservoir Testing: 1978 to 1980." *Journal of Volcanology and Geothermal Research*, Geothermal Energy of Hot Dry Rock, 15 (1):59–99. [https://doi.org/10.1016/0377-0273\(83\)90096-3](https://doi.org/10.1016/0377-0273(83)90096-3).
- Duguid, James O., and P. C. Y. Lee. 1977. "Flow in Fractured Porous Media." *Water Resources Research* 13 (3):558–66. <https://doi.org/10.1029/WR013i003p00558>.
- Fakcharoenphol, Perapon, Yi Xiong, Litang Hu, Philip H. Winterfeld, Tianfu Xu, and Yu-Shu Wu. 2013. "User's Guide of Tough2-Egs. a Coupled Geomechanical and Reactive Geochemical Simulator for Fluid and Heat Flow in Enhanced Geothermal Systems Version 1.0." DOE-CSM--0002762-1. Colorado School of Mines, Golden, CO (United States). <https://doi.org/10.2172/1136243>.
- Karimi-Fard, M., L.J. Durlofsky, and K. Aziz. 2003. "An Efficient Discrete Fracture Model Applicable for General Purpose Reservoir Simulators." In . Society of Petroleum Engineers. <https://doi.org/10.2118/79699-MS>.
- Kazemi, H. 1969. "Pressure Transient Analysis of Naturally Fractured Reservoirs with Uniform Fracture Distribution." *Society of Petroleum Engineers Journal* 9 (04):451–62. <https://doi.org/10.2118/2156-A>.
- Lee, S. H., M. F. Lough, and C. L. Jensen. 2001. "Hierarchical Modeling of Flow in Naturally Fractured Formations with Multiple Length Scales." *Water Resources Research* 37 (3):443–55. <https://doi.org/10.1029/2000WR900340>.
- Computer Modeling Group Ltd. 2012. "CMG-STARS User's Guide," January.

- Moinfar, Ali, Abdoljalil Varavei, Kamy Sepehrnoori, and Russell T. Johns. 2014. "Development of an Efficient Embedded Discrete Fracture Model for 3D Compositional Reservoir Simulation in Fractured Reservoirs." *SPE Journal* 19 (02):289–303. <https://doi.org/10.2118/154246-PA>.
- Murphy, Hugh D. 1979. "Heat Production On From A Geothermal Reservoir Formed By Hydraulic Fracturing - Comparison Of Field And Theoretical Results." In . Society of Petroleum Engineers. <https://doi.org/10.2118/8265-MS>.
- Pruess, K., and R. C. Schroeder. 1980. "Shaft79 User's Manual." LBL-10861. California Univ., Berkeley (USA). Lawrence Berkeley Lab. <https://doi.org/10.2172/5355427>.
- Pruess, K., and Y. S. Wu. 1988. "On Pvt-Data, Well Treatment, and Preparation of Input Data for an Isothermal Gas-Water-Foam Version of Mulkom." LBL-25783. Lawrence Berkeley Lab., CA (USA). <https://www.osti.gov/scitech/biblio/6121230>.
- Pruess, Karsten, C. M. Oldenburg, and G. J. Moridis. 1999. "TOUGH2 User's Guide Version 2." *Lawrence Berkeley National Laboratory*. <http://escholarship.org/uc/item/4df6700h.pdf>.
- Sadrpanah, Hooman, Thierry Charles, and Jonathan Fulton. 2006. "Explicit Simulation of Multiple Hydraulic Fractures in Horizontal Wells." In . Society of Petroleum Engineers. <https://doi.org/10.2118/99575-MS>.
- SCHLUMBERGER, ECLIPSE User Manual. "Technical Description." *Schlumberger Ltd* (2009).
- Settari, A., and Dale A. Walters. 2001. "Advances in Coupled Geomechanical and Reservoir Modeling With Applications to Reservoir Compaction." *SPE Journal* 6 (03):334–42. <https://doi.org/10.2118/74142-PA>.
- Slough, K. J., E. A. Sudicky, and P. A. Forsyth. 1999. "Grid Refinement for Modeling Multiphase Flow in Discretely Fractured Porous Media." *Advances in Water Resources* 23 (3):261–69. [https://doi.org/10.1016/S0309-1708\(99\)00009-3](https://doi.org/10.1016/S0309-1708(99)00009-3).
- Sun, Jianlei, and David Stuart Schechter. 2014. "Optimization-Based Unstructured Meshing Algorithms for Simulation of Hydraulically and Naturally Fractured Reservoirs with Variable Distribution of Fracture Aperture, Spacing, Length and Strike." In . Society of Petroleum Engineers. <https://doi.org/10.2118/170703-MS>.
- Vinsome, P. K. W., and J. Westerveld. 1980. "A Simple Method For Predicting Cap And Base Rock Heat Losses In' Thermal Reservoir Simulators." *Journal of Canadian Petroleum Technology* 19 (03). <https://doi.org/10.2118/80-03-04>.
- Wang, Cong, Xiaoping Mao, and Yu-Shu Wu. 2017. "A General Three-Dimensional Embedded Discrete Fracture Method for Reservoir Simulation with Complicated Hydraulic Fractures." *SPE Journal*.
- Warren, J. E., and P. J. Root. 1963. "The Behavior of Naturally Fractured Reservoirs." *Society of Petroleum Engineers Journal* 3 (03):245–55. <https://doi.org/10.2118/426-PA>.
- Wu, Y.-S., C. Ehlig-Economides, Guan Qin, Zhijiang Kang, Wangming Zhang, Babatunde Ajayi, and Qingfeng Tao. 2007. "A Triple-Continuum Pressure-Transient Model for a Naturally Fractured Vuggy Reservoir." *Lawrence Berkeley National Laboratory*, August. <http://escholarship.org/uc/item/8fr0m0pp>.